COBEM 2021 26th International Congress of Mechanical Engineering
November 22-26, 2021, Virtual Congress, Brazil
ABCM Associação Brasileira de Engenharia e Ciências Mecânicas

COB-2021-1710
MODELING OF THE PARABOLIC KICK DEVICE OF OMNIDIRECTIONAL ROBOTS

Eric Ezequiel Yoshida de Lima
Daniela Vacarini de Faria
Reynaldo Santos de Lima
Luiz Carlos Sandoval Góes
Mechanical Engineering Division, Aeronautics Institute of Technology - São José dos Campos / SP
eric_lima20@yahoo.com, danivacarini@gmail.com, goes@ita.com, reynaldo.sdlima@gmail.com

Marcos R. O. A. Maximo
Autonomous Computational Systems Lab (LAB-SCA),
Computer Science Division, Aeronautics Institute of Technology - São José dos Campos / SP
mmaximo@ita.br

Abstract. *RoboCup is an international robotics competition to foster robotics and artificial intelligence research. In the RoboCup Small Size League (SSL), two teams of eleven (Division A) or six (Division B) physical omnidirectional robots compete in a soccer match. The teams typically develop their robot hardware, which is endowed by kicking mechanisms: the so-called kicker and chip kicker (chipper), which execute low and high kicks, respectively. In this paper, we simulate and optimize the chipper of our team ITAndroids' robot. Our chipper is a mechanism based on the acceleration of a piston, due to the magnetic field of a solenoid, which in turn collides with the chipper and perform the oblique launch of the ball. In this regard, our contribution is two-fold. First we show the equations that govern the dynamic system and how to implement them in a simulation using MATLAB and Simulink. After simulating the dynamical system, we noticed that it is possible to adjust the trajectory of the ball according to the time interval that the circuit is energized, which can be used for accurate kicks. Second, metaheuristic optimization was used by means of evolutionary strategies to obtain the best chipper geometry to improve the efficiency of the system, respecting the physical restrictions. To perform the optimization, the CMA-ES algorithm and a simple evolutionary strategy (SES) were used. A comparison of the two algorithms was carried out, and it was possible to observe that, due to the relative complexity of the problem, the CMA-ES, which is a more complete algorithm, obtained a better final result than the SES. The optimized design represents a considerable improvement (approximately 40%) from the current chipper used in our robot. The proposed methodology may benefit other SSL teams and serve as a guide for simulating and optimizing other electromechanical devices.*

Keywords: *chipper, kick, mechanics, robotics, optimization, CMA-ES*

1. Introduction

It is noticeable that the robotics area has been constantly developing over the years. In this sense, with the intention of encouraging research in the area, international robotics competitions emerged, such as the RoboCup (Kitano, Asada, Kuniyoshi, Noda, Osawa and Matsubara, 1997), a robot soccer competition, in which autonomous robots are capable to play matches without any human intervention. With the purpose of creating a robot soccer category in which, in addition to speed, there is also the possibility of cooperation between robots, Small Size was created within RoboCup (RoboCup, 1997). With that, in order to develop better cooperation between robots, over the years, new mechanisms have emerged, such as different types of kicks to propel the ball. The current robots in the category move omnidirectionally, i.e., they allow movements in any direction, and are capable of performing low and high kicks through mechanisms called, respectively, Kicker and Chipper.

In this context, the presence of the "chip kicker" mechanism is essential, given that it allows for a greater number of strategic opportunities in competition games. Such a mechanism can be implemented with different types of devices, e.g., hydraulic, pneumatic or electrical mechanisms. The chosen system was the electric one (Zandsteeg and van de Molengraft, 2005), which is based on the solenoid actuator model, since this system provides greater efficiency and ball movement control, in addition to being more compact.

In this paper, the mathematical modeling and the development of a chipper design considering the electromechanical effects were presented. Furthermore, the optimization of the mechanical parameters of the chipper was presented, using well-established computational optimization techniques. In this sense, it was possible to obtain a geometry for the part

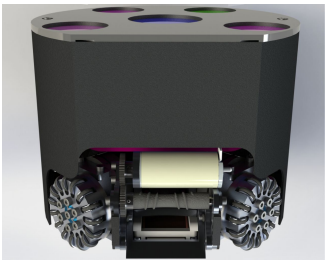

(a) ITAndroids project for the Small Size category.

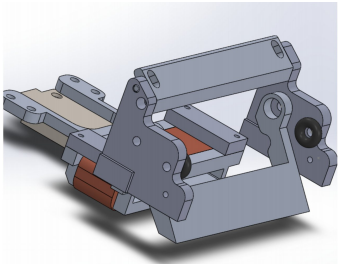

(b) Chipper mechanism with solenoid actuator.

Figure 1: Small Size robot and a Chipper mechanism.

that maximizes its performance, which shows the efficiency of computational optimizations in solving some mechanics problems.

Some works, such as Meessen, Paulides and Lomonova (2010) and Lima (2019), develop the electromechanical model in a similar way to the one developed in this paper. In addition, other works, such as Koopai, Ghasemieh, Khanloghi, Mohammadi, Matin and Torabian (2019), present ideas similar to those of this paper in regards to the performance of chipper optimization, but do not use computational optimization algorithms, something that was implemented and discussed in this work.

The rest of this paper is organized as follows. Section 2 describes the problem to be studied. Section 3 presents and discusses the results obtained from the simulations and optimizations. Finally, Section 4 concludes and submits ideas for future works.

2. Problem Description

The project consisted of the development of a parabolic kick mechanism for soccer coverage plays by omnidirectional robots of the RoboCup Small Size League (RoboCup, 1997). Firstly, a literature review was carried out on papers from other Small Size teams that have already participated in world competitions, in order to find out what is the best type of mechanism to be used. Subsequently, the functioning of the adopted mechanism was studied and, then, tests and simulations of the system were carried out in the MATLAB and Simulink softwares (MATLAB and Simulink Toolbox Release 2019b). In this way, it was possible to obtain the desired information, such as the ball's velocity, the distance covered, and the maximum height reached.

With the information obtained through the simulations, the best geometries and components for the chipper modeling were studied using optimization techniques. Then, the parts would be manufactured to carry out operational tests of the new components on the prototype robot. However, due to the COVID-19 pandemic, it became impracticable to carry out such tests, which will be carried out when academic activities resume normally.

2.1 Description of the solenoid actuator functioning

It is noticeable that to perform the analysis of the solenoid actuator (Cheung, Lim and Rahman, 1993), one must fully understand the electromechanical system. In this sense, in order to facilitate the description of the adopted model, this system was divided into parts, to later unite them as a single mechanism.

2.1.1 The system's power supply

For the solenoid actuator plunger to be accelerated, it is necessary to generate a variation in the magnetic field in regards to time inside the actuator (Halliday, Resnick, Walker and Romo, 1986). Such variation occurs through the passage, along the solenoid, of an electrical current that varies with time. In this sense, it is possible to analyze the factors that influence this circuit in order to optimize the impulse generated in the solenoid plunger.

It is known that to generate a large variation of electrical current along the solenoid, it is necessary that the system's power supply supplies current to the circuit in an immediate manner. Thus, a capacitor was used, as it is capable of generating a voltage spike at the moment it is connected to the circuit (Nussenzveig, 2015). Therefore, the circuit is composed of a capacitor that is charged by a voltage source connected in parallel, in the position 1 of the switch, and a capacitor in series with the solenoid and an internal resistance for activation in the position 2 of the switch. In this sense, from Fig. 2a, it can be noted that it is possible to manage the velocity of the plunger through the time interval in which the plunger is exposed to the variation of the magnetic field. Therefore, it suffices to define the time interval in which the switch is in the position 2 to control the plunger's velocity.

Notice that from a brief analysis of the RLC circuit in Fig. 2a, that the only values of the circuit that remain variable

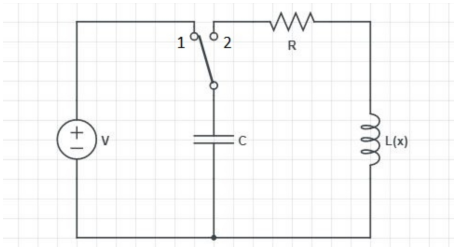

(a) RLC circuit with capacitor connected in parallel to the voltage source.

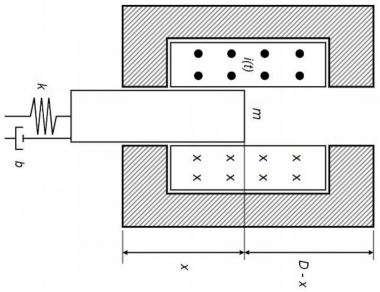

(b) Solenoid actuator section view.

Figure 2: Magnetic circuit of the system.

over time are the electric current and the inductance of the solenoid. However, through the theory of RLC circuits (Nussenzveig, 2015), it is possible to determine the current from other quantities. Thus, it is essential to understand the inductance behavior to be able to reach the final goal, which is the determination of the plunger's velocity over time.

2.1.2 Magnetic circuit analysis

Firstly, in order to be able to determine the plunger's velocity, it is necessary to analyze the circuit's inductor. In this sense, to carry out the study of the solenoid, the system was simplified, by disregarding the reluctance of air in the lateral gaps between the plunger and the solenoid. Therefore, it was considered that the section area of the plunger is equal to the section area of the solenoid's interior.

Firstly, from Fig. 2b, it is possible to analyze the RLC circuit, in which it is already possible to relate the electric potential to the inductance of the solenoid. As described in Kingsley Jr, Umans and Fitzgerald (2006):

$$U(t) = \frac{q(t)}{C}, \tag{1}$$

in which U is the capacitor's voltage, q is the charge stored, and C is the capacitance. In addition, we have:

$$U(t) = Ri(t) + \frac{d\lambda}{dt}, \tag{2}$$

in which R is the electrical resistance, $i(t)$ is the current (as a function of time), and λ is the magnetic flux that is described as:

$$\lambda(t) = i(t)L(x(t)), \tag{3}$$

where $L(x(t))$ is the inductance of the solenoid, where $x(t)$ is the distance (also variable with time) of the plunger inserted in the solenoid. Thus, from equations (1), (2) and (3), we have that:

$$\frac{di(t)}{dt} = \frac{q(t)}{CL(x(t))} - \frac{Ri(t)}{L(x(t))} - i(t)\frac{dx(t)}{dt}\frac{dL(x)}{dx}\frac{1}{L(x(t))}. \tag{4}$$

Furthermore, from Fig. 2b, knowing that the reluctance of air on the lateral gaps was disregarded, the reluctance of the system will refer to the part of the plunger inside the solenoid and to the part of the solenoid filled with air. Thus, from the solenoid inductance Eq. (Halliday, Resnick, Walker and Romo, 1986), we have:

$$L(x(t)) = \frac{\mu_o N^2 A}{\frac{x(t)}{\mu_R} + D - x(t)}, \tag{5}$$

in which μ_o is the magnetic permeability of the air, N is the number of coils, A is the cross-sectional area of the solenoid, μ_R is the relative magnetic permeability of the plunger, and D is the length of the solenoid. As the length of the plunger is greater than that of the solenoid, the scenario in which the plunger is completely inside the solenoid was not considered in the calculations. Furthermore, as the 'chipper' part is positioned immediately after the solenoid, the scenario in which the plunger is coming out of the solenoid was also not considered, given that when it starts to come out it will collide with the chipper.

Then, it is necessary to relate the mechanisms of the spring and the damper coupled to the plunger, in order to understand the functioning of the system. Such mechanisms are responsible for making the plunger return to the initial

position. To this end, we must, first, analyze the energy E of the inductor, which according to Kingsley Jr, Umans and Fitzgerald (2006), is given by:

$$E = \frac{L(x(t))i(t)^2}{2}. \tag{6}$$

Thus, it is concluded that the force, due to the variation of the magnetic field, generated in the plunger, is given by:

$$F = \frac{i(t)^2}{2}\frac{dL(x)}{dx}. \tag{7}$$

After that, the analysis of the mechanical system is performed, in order to relate the mechanical part to the electrical part of the system.

2.1.3 Mechanical system

From Fig. 2b, one may notice the presence of a spring of elastic constant k, responsible for returning the plunger to the original position. In addition to this component, to represent a possible friction between the plunger and the solenoid, a damper with a damping constant b was illustrated in the assembly. Thus, it becomes possible to relate such components with the electrical system through Newton's 2nd Law, as described in Halliday, Resnick, Walker and Romo (1986). That way, one has that:

$$\frac{dv(t)}{dt} = \frac{i(t)^2}{2m}\frac{dL(x)}{dx} - \frac{kx}{m} - \frac{bv(t)}{m}. \tag{8}$$

Notice that Eq. (8) describes the behavior of the forces acting on the plunger. Thus, from the equations described, it is possible to analyze the system as the union of the electromagnetic circuit with the mechanical system, so that the analysis of a single system can be performed.

2.1.4 Electromechanical system

Through the equations obtained, notice that the solenoid actuator is now seen as a single electromechanical system. However, to complete the analysis of the dynamical system, there is still a need for two basic equations, which reduce the number of variables. Thus, one has that:

$$i(t) = -\dot{q}(t), \tag{9}$$

$$v(t) = \dot{x}. \tag{10}$$

It is noticeable that the system composed by equations (4), (5), (8), (9) and (10) is sufficient to analyze the kick mechanism in relation to time. In this sense, understanding the functioning of such a mechanism facilitated the development of the simulation in Simulink (MATLAB and Simulink Toolbox Release 2019b). That way it was possible to obtain the plunger's velocity at any instant of time by assembling the solenoid actuator system in Simulink.

2.2 Description of the chip-kicker's functioning

Upon completion of the step of acceleration of the plunger in the solenoid actuator, the chip kicker component will become part of the dynamic system. In this sense, it is necessary to analyze the movement in order to understand what will be the exit velocity of the ball.

2.2.1 Plunger collision analysis

In Fig. 3, notice that after the plunger exits the interior of the solenoid, it will collide with the chip kicker. To simplify the system, some simplifications will be considered. One of them will be the fact that the collision between the plunger and the chip kicker is elastic, that is, the energy during the collision will be conserved. First, to perform the analysis of this system, it is noted that there is no external torque being performed on the mechanism during the collision. In this way, the angular momentum of the system is conserved during impact (Nussenzveig, 2018). Furthermore, it is noticed that the total energy of the system is also conserved. Thus, one has that:

$$md_y v_1 = I\omega + md_y v_2, \tag{11}$$

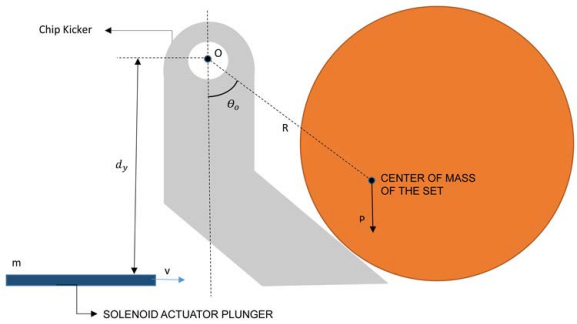

Figure 3: Schematic drawing of the Chipper's functioning.

$$\frac{mv_1^2}{2} = \frac{I\omega^2}{2} + \frac{mv_2^2}{2}, \tag{12}$$

in which v_1 is the velocity of the plunger before the collision, v_2 is the velocity of the plunger after the collision, d_y is the distance between the plunger and axis O, and I is the moment of inertia of the ball-chip kicker set with respect to axis O, which is obtained through Steiner's Theorem (Nussenzveig, 2018):

$$I = I_{CM} + MR^2, \tag{13}$$

in which R is the perpendicular distance between the two axes (axis O and the axis parallel to it and passing through the center of mass) and M is the total mass of the set. It is noticeable that, from equations (11) and (12), the angular velocity acquired by the ball-chip kicker set is obtained:

$$\omega = \frac{2v_1}{d_y\left(\frac{I}{md_y^2} + 1\right)}. \tag{14}$$

In Fig. 3, after the collision, notice that the chip kicker begins a rotational motion with a deceleration. Therefore, after that, the analysis of the system is carried out along this movement, to determine the ball's final velocity.

2.2.2 Analysis of rotational motion

From Fig. 3, after the collision, it can be seen that the ball starts to perform a rotational motion, around axis O, ascending, in relation to the ground. However, due to the torque of the weight force of the ball-chip kicker set, there is an angular deceleration $-\alpha$. Thus, to determine the exit velocity of the ball, it is necessary to understand such deceleration $-\alpha$. By adapting Newton-Euler Equations to rotational systems (Halliday, Resnick, Walker and Romo, 1986), one has that:

$$MgRsen\theta = -I\alpha. \tag{15}$$

In Eq. (15), it was considered that the friction existing in the rotation axis is negligible, since a high-quality bearing is being used to reduce the friction at this point. In addition, according to Eq. (15), there is a deceleration $-\alpha$ dependent of the angular position of the set. In this sense, to solve such a system, it sufficed to assemble a simple simulation in Simulink (MATLAB and Simulink Toolbox Release 2019b), in order to obtain the final ball exit velocity. Thus, it suffices to finish the analysis by determining the reach attained as well as the height reached at throw.

2.2.3 Oblique Throw

It is observed that when obtaining the exit velocity of the ball, in addition to having knowledge of the throw angle, it becomes possible to describe the movement performed by the ball. Therefore, as described in (Nussenzveig, 2018), one has that:

$$S = \frac{v_o^2 sen(2\theta)}{g}, \tag{16}$$

$$H_{max} = \frac{v_o^2 sen^2\theta}{2g}. \tag{17}$$

in which S and H_{max} are respectively the distance travelled and the maximum height reached by the ball, v_o is the exit velocity of the ball, θ is the angle the velocity vector makes with the horizontal and g is the acceleration of gravity.

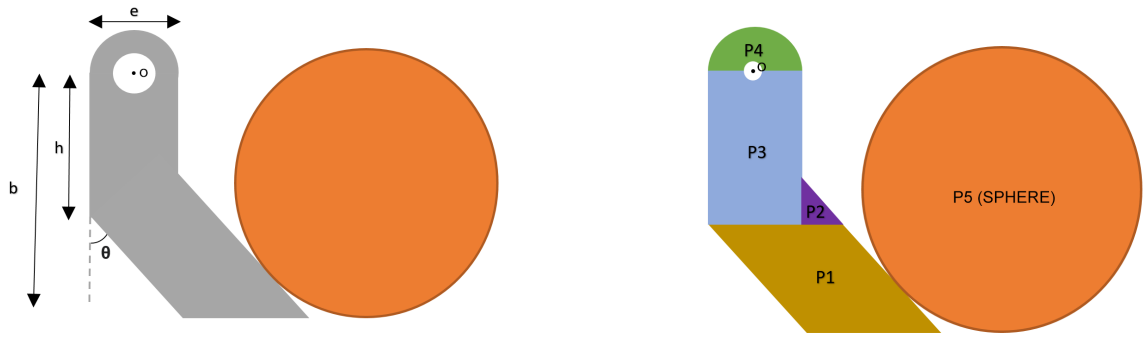

(a) Chipper scheme with the parameters used in the optimization.

(b) Chipper parts division.

Figure 4: Optimization parameters and chipper division.

2.3 Chipper Geometry Optimization

Firstly, to analyze this problem, we studied the geometric part of the Chipper to define the objective function of the optimization. Subsequently, a simple evolution strategy (SES), which is a method that adapts the mean and covariance calculated based on the best λ samples of the generation, was implemented, in Python, to optimize the chip kicker geometry, and compared using the CMA-ES implementation (*Covariance Matrix Adaptation Evolution Strategy*) (Hansen, 2016), which was obtained from the $pycma$ library (Hansen, Akimoto and Baudis, 2019).

2.3.1 Definition of the Objective Function from the Chipper Geometry

It is noticeable, from Eq. (14), that the velocity acquired by the Chipper can be maximized by minimizing the term $\gamma = I/d_y$ in the denominator. Thus, the objective function used in the optimization was the term γ. To enable the implementation of the objective function, it is necessary to calculate the moment of inertia. After studying the part, it is clear that four parameters are needed to completely define the Chipper, which are the height h, total height b, thickness e, and inclination angle θ, as shown in Fig. 4a. Once we have the necessary parameters to define the part, it suffices to calculate the moment of inertia of the part in relation to axis O. For this, the part was divided into five sections, as described in Fig. 4b, and the moment of inertia was calculated for each part with regards to their respective centers of mass. Finally, through Steiner's Theorem (Nussenzveig, 2018), the moment of inertia of each part with regards to axis O was obtained. For the 1st section (trapezoidal section) of the part, one has that:

$$I_1 = \frac{1}{12}\rho abc(a^2 + b^2(\tan^2\theta + 1)). \tag{18}$$

in which a is the base, b is the height, c is the depth, and ρ is the density of the part's section.

For the 2nd section (triangular section) of the part, one has that:

$$I_2 = \frac{1}{36}\rho abc(a^2 + b^2). \tag{19}$$

For the 3rd section (rectangular section) of the piece, one has that:

$$I_3 = \frac{1}{12}\rho abc(a^2 + b^2). \tag{20}$$

For the 4th section (semi-circular) of the part, one has that:

$$I_4 = \frac{1}{4}\rho\pi cR^4. \tag{21}$$

As the 5th part is a spherical ball, the moment of inertia of the sphere is:

$$I_5 = \frac{2}{5}mr^2. \tag{22}$$

With the mass and the distance from the center of mass of each part to the axis O, it is possible to obtain, through Steiner's Theorem (Nussenzveig, 2018), the moment of inertia of the part with respect to the axis O. Thus, it was possible to implement the objective function of the CMA-ES, which is first calculated with the term $\gamma = I/d_y$. Furthermore, in optimizations based on evolution strategies, it is common to add constraints to the variables so that the algorithm does

not find unwanted solutions (Depinet, MacAlpine and Stone, 2014). In this sense, in order to avoid cases in which the algorithm results in physically impossible dimensions, for example negative dimensions, such constraints were added to the objective functions when the algorithm obtains such results. Also, as CMA-ES does not allow constraints, these constraints were added through an addition of high cost in the cost function. These mechanical constraints are summarized in well-defined limits of values for which the parameters can vary, in order to avoid generating parts that are impossible to manufacture.

2.3.2 Implementation of SES and CMA-ES

For the implementation of the optimization, the official CMA-ES implementation interface was used (Hansen, Akimoto and Baudis, 2019), adopting the standard strategy in which $\mu = 3$ and $\lambda = 6$, where μ is the number of parents used to compute the mean and covariance of the next generation and λ is the population size. For more information on evolution strategies, we recommend reading Hansen's tutorial (Hansen, 2016). In addition, for the objective function, four parameters were used, which were: height h, height b, thickness e, and inclination angle θ (see Fig. 4a), returning the value of the moment of inertia divided by the total height of the part. Furthermore, to be able to compare the performance of the CMA-ES algorithm, an SES algorithm was also implemented, using a strategy in which $\mu = 75$ and $\lambda = 150$, as well as the creation of a benchmark capable of testing and comparing the algorithms.

3. Results and Discussions

As already mentioned, the goal of this project is to study the movement described by the ball when using a high kick mechanism. In this sense, according to the equations presented, it was found that it is possible to choose the values of reach and height by choosing the time interval in which the switch is kept in positions 1 and 2.

Thus, a simulation of a model was performed, so that, through a time interval entry, it is possible to control the distance and height that will be covered by the ball. To carry out the simulations, the current Chipper model, developed at ITAndroids (Lima, 2019), was used as a basis. The simulation of the developed model was made available as open source for the community[1].

3.1 Solenoid actuator simulation

Firstly, based on (Lima, 2019), from equations (4), (8), (9) and (10), a model was built, in a block diagram, in Simulink (MATLAB and Simulink Toolbox Release 2019b). Therefore, to include the model equations in Simulink, a block called MATLAB Function was used, where the corresponding equations were inserted, using as state variables:

$$[q(t), \dot{q}(t), x(t), \dot{x}(t)]^T,$$

and as output variables, their derivatives:

$$[i(t), \dot{i}(t), v(t), \dot{v}(t)]^T,$$

In this way, an interactive system is obtained, in which integrations are performed at each cycle, until the moment when the plunger is on the verge of reaching the chip kicker. For this, a Switch block was used, in which the velocity is canceled if the plunger reaches a certain position (base of the chip kicker). Furthermore, in order to understand the behavior of the plunger's velocity and of the charge stored in the capacitor, blocks were used to analyze these parameters as a function of time. Moreover, in this simulation, we used the parameters of the 'chipper' that currently exists in ITAndroids. Such simulations are configured with the Simulink version 10.0's standard.

From Fig. 5a, it can be seen that the maximum velocity reached by the plunger was $5\,\mathrm{m/s}$. In this sense, in order to understand the maximum reach and maximum height reached by the ball, the mentioned value was used to simulate the movement of the chip kicker.

3.2 Chip Kicker simulation

First, from the SolidWorks software, it was possible to determine the moment of inertia of the system around the axis O:

$$I = 49806\,\mathrm{g\,mm^2}.$$

Therefore, the angular velocity value of the assembly after the collision was calculated, using the plunger's velocity of $5\,\mathrm{m/s}$ (the highest possible):

$$\omega \approx 310\,\mathrm{rad/s}.$$

[1]The implemented simulation can be found on the link `https://gitlab.com/itandroids/open-projects/ssl-chipper-mechanism-simulator/-/tree/main/simulation`.

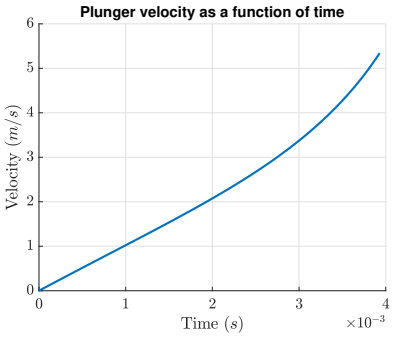

(a) Plunger velocity as a function of capacitor discharge time.

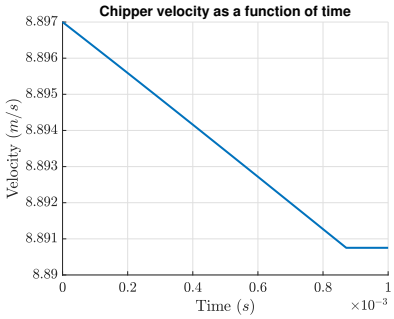

(b) Velocity of the ball + chip kicker as a function of time.

Figure 5: Plunger and chipper velocity as a function of time.

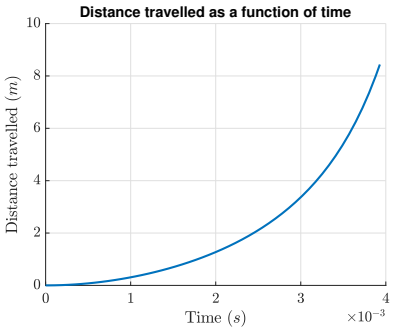

(a) Distance covered as a function of capacitor discharge time.

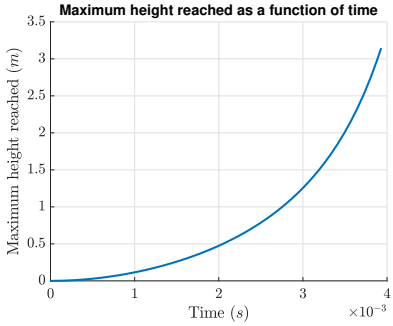

(b) Height reached as a function of capacitor discharge time.

Figure 6: Distances and heights travelled as a function of capacitor discharge time.

Thus, from the values of the moment of inertia I and the angular velocity ω, it was possible to proceed with the elaboration of block diagrams in Simulink, in order to carry out the simulation. From Eq. (15), a MATLAB function was defined, in which the input parameter was the angle of the center of mass with the vertical, and the output parameter was the angular deceleration of the set. In the block diagram assembled in Simulink (MATLAB and Simulink Toolbox Release 2019b), it can be seen that the system will remain in a cycle with integration relations, until the moment the chip kicker reaches the stopper. To limit the mechanism, a Switch was inserted, so that, if the angle exceeded a certain value, the simulation would end. Furthermore, a block was used to analyze the behavior of the ball's velocity during the movement. From the graph shown in Fig. 5b, we obtain the value of the ball's throwing velocity, which is approximately $8.89\,\mathrm{m/s}$. It is noticeable that the influence of the weight force torque on the mechanism is very low, given that the variation in velocity is small. This fact is due to the short time interval (approximately $1.2\,\mathrm{m/s}$) in which the system is subjected to deceleration torque, which is also not excessively big.

3.3 Oblique Throw

Starting from the throw angle, combined with the velocity of the throw obtained in the simulation, the oblique throw of the ball can be clearly described. From equations (16) and (17), one has that:

$S_{max} \approx 7.3\,\mathrm{m}$ and $H_{max} \approx 2.7\,\mathrm{m}$.

However, knowing that the system deceleration is very small, it can be disregarded in the calculation of velocity. In this way, equations (14), (16) and (17) can be added to the solenoid actuator simulation, so that it becomes possible to analyze the behavior of the distance and height covered as functions of the time interval in which the capacitor is discharging. To carry out this analysis, the highlighted equations were inserted within the MATLAB function, and the outputs D and H were added, which are the distance and the height covered, respectively. Furthermore, to be able to understand the behavior of such outputs, as a function of time, blocks of analysis were added. Finally, it is possible to verify in Figures 6a and 6b that the maximum values of the distance and height of the new simulation do not differ much from the values of S_{max} and H_{max}, obtained when considering the torque of the weight force, which shows that such an approximation is viable. In addition, such curves of distance and height travelled by the ball as functions of the time interval that the capacitor keeps discharging, seen in Figures 6a and 6b, are very important for the strategy team to be able to predict the ball's trajectory and thus control the chipper more accurately.

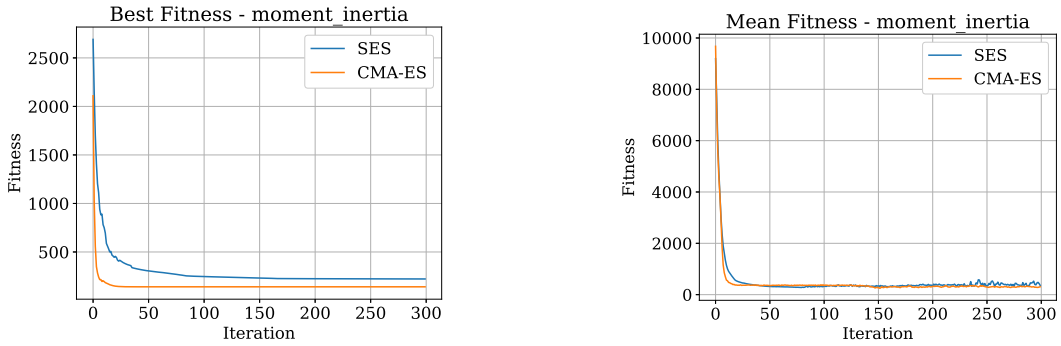

(a) Best fitness for the objective function.

(b) Mean fitness for the objective function.

Figure 7: Objective function fitness graphs.

3.4 Chipper Optimization

After running CMA-ES several times, it was observed that the algorithm reaches the global minimum in most of the optimizations. By analyzing the values obtained, it was found that the best option to optimize it is maximizing the parameters up to the limit imposed on mechanical constraints.

In this sense, in order to make a comparison between the optimized chipper and the old ITAndroids chipper, a file with the *.py extension was created, which provides the percentage of improvement of the factor $\gamma = I/d_y$. Running this file, with the data of the best result generated by the optimization of the CMA-ES, it was found that there was an improvement of 41.1% compared to the old chipper. The codes for this optimization were made available as open source to the community[2].

Furthermore, in order to compare the results of CMA-ES with those of a different method, optimization was performed using the Simple Evolution Strategy (SES). In this sense, the implementation of the SES required an increase in the population in relation to the CMA-ES to reduce the chance of it getting stuck into bad local minima. However, it was observed that, even with the population increase, using the SES, the algorithm tends to get stuck into local minima in most cases, which results in lower performance when compared to CMA-ES. Furthermore, to better validate such observed fact, the two algorithms were compared by a benchmark using Monte Carlo simulations. In Fig. 7a, it can be seen that the CMA-ES is able to reach the global optimum, while the SES converges to a local optimum. In Fig. 7b, it can be seen that, on average, the algorithms converge to the same optimal location. Moreover, the Simulink simulations were run again (MATLAB and Simulink Toolbox Release 2019b), using the parameters of the new optimized Chipper[3]. From Figures 8a and 8b, it can be seen that there is a considerable increase both in the distance travelled and in the maximum height reached:

$$S_{max} \approx 10.2\,\mathrm{m} \text{ and } H_{max} \approx 3.8\,\mathrm{m}.$$

an increase of 39.7% for the maximum distance covered and an increase of 40.7% for the maximum height reached, which demonstrates great improvement in comparison to the old Chipper.

4. Conclusion

From the theoretical analysis of the described electromechanical mechanism, it was possible to assemble a simulation capable of satisfactorily representing the proposed system. In addition, through simulation, performed with a block diagram in Simulink (MATLAB and Simulink Toolbox Release 2019b), it was possible to build a direct relation of the oblique ball throw parameters with the time interval in which the capacitor is maintained discharging into the circuit. In this way, a much simpler and more precise mechanism is created to control the positioning the ball will reach after a throw. Furthermore, it is clear that such analysis enabled the team in the Small Size category (RoboCup, 1997), ITAndroids, ITA's robotics team, to develop an essential component to be used in matches between robots. In this way, a greater variety of strategies and moves became possible for the team, making it even more competitive in national and international competitions in the category. It is also noted, from the theoretical analysis of the geometry of the studied part, that it was possible to develop an optimization capable of significantly improving the part in question, which shows the efficiency of optimization algorithms in mechanical problems. Thus, it could be verified that, in view of the percentage of improvement

[2]Optimization codes can be found on the link `https://gitlab.com/itandroids/open-projects/ssl-chipper-mechanism-simulator/-/tree/main/evolution_strategy`.

[3]The optimized chipper technical design can be found on the link `https://gitlab.com/itandroids/open-projects/ssl-chipper-mechanism-simulator/-/blob/main/chipper_technical_design.PDF`.

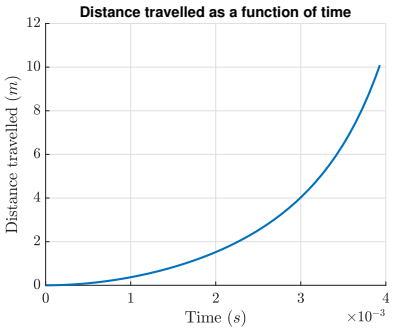

(a) Distance travelled as a function of capacitor discharge time for the optimized Chipper.

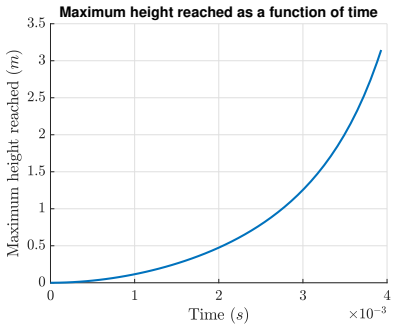

(b) Height reached as a function of capacitor discharge time for the optimized Chipper.

Figure 8: Distances and heights travelled as a function of capacitor discharge time for the optimized Chipper.

achieved, the optimization was successful. Finally, some perspectives for future work are the making and assembling of the chipper, as well as experimental testing to validate the theoretical model.

5. ACKNOWLEDGEMENTS

The author Eric Lima would like to thank the CNPQ (National Council for Scientific and Technological Development) for the scientific initiation scholarship offered. Furthermore, the authors would like to thank the entire ITAndroids team for their great help during the project and ITAex. Finally, the authors thank the other ITAndroids sponsors: Altium, Cenic, Intel, MathWorks, Metinjo, Micropress, Polimold, Rapid, SolidWorks, STMicroelectronics, Wildlife Studios and Virtual.PYXIS for the support given to students and staff.

6. REFERENCES

Cheung, N., Lim, K. and Rahman, M., 1993. "Modelling a linear and limited travel solenoid". In *Proceedings of IECON'93-19th Annual Conference of IEEE Industrial Electronics*. IEEE, pp. 1567–1572.

Depinet, M., MacAlpine, P. and Stone, P., 2014. "Keyframe sampling, optimization, and behavior integration: Towards long-distance kicking in the robocup 3d simulation league". In *Robot Soccer World Cup*. Springer, pp. 571–582.

Halliday, D., Resnick, R., Walker, J. and Romo, J.H., 1986. *Fundamentos de física*. QC23. H35 2007. Compañía Editorial Continental.

Hansen, N., 2016. "The cma evolution strategy: A tutorial". *arXiv preprint arXiv:1604.00772*.

Hansen, N., Akimoto, Y. and Baudis, P., 2019. "CMA-ES/pycma on Github". Zenodo, DOI:10.5281/zenodo.2559634. doi:10.5281/zenodo.2559634. URL `https://doi.org/10.5281/zenodo.2559634`.

Kingsley Jr, C., Umans, S.D. and Fitzgerald, A.E., 2006. *Máquinas Elétricas-: Com Introdução à Eletrônica de Potência*. Bookman.

Kitano, H., Asada, M., Kuniyoshi, Y., Noda, I., Osawa, E. and Matsubara, H., 1997. "Robocup: A challenge problem for ai". *AI Magazine*, Vol. 18, No. 1, p. 73. doi:10.1609/aimag.v18i1.1276. URL `https://aaai.org/ojs/index.php/aimagazine/article/view/1276`.

Koopai, O.N., Ghasemieh, M., Khanloghi, M., Mohammadi, A., Matin, A. and Torabian, A., 2019. "Immortals 2019 extended team description paper".

Lima, R., 2019. "Modelagem de mecanismo eletromecânico de chute de futebol de robôs". *ITAndroids*.

MATLAB and Simulink Toolbox Release 2019b, 2019. The MathWorks, Natick, MA, USA.

Meessen, K., Paulides, J. and Lomonova, E., 2010. "A football kicking high speed actuator for a mobile robotic application". In *IECON 2010-36th Annual Conference on IEEE Industrial Electronics Society*. IEEE, pp. 1659–1664.

Nussenzveig, H.M., 2015. *Curso de física básica: Eletromagnetismo*, Vol. 3. Editora Blucher.

Nussenzveig, H.M., 2018. *Curso de Física Básica: fluidos, oscilações e ondas, calor*, Vol. 2. Editora Blucher.

RoboCup, 1997. *RoboCupSoccer - Small Size*. URL: `https://www.robocup.org/leagues/7`.

Zandsteeg, C. and van de Molengraft, I.M., 2005. "Design of a robocup shooting mechanism". *University of Technology Eindhoven*, p. 44.

7. RESPONSIBILITY NOTICE

The authors are solely responsible for the printed material included in this paper.